Theoretical insights on the mechanism of alkene epoxidation by H_2O_2 with titanium silicalite

Matthew Neurock*[a] and Leo E. Manzer[b]

[a] *Department of Chemical Engineering, University of Virginia, Charlottesville, VA 22903-2442, USA*
[b] *DuPont Central Research and Development, Experimental Station, Wilmington, DE 19880-0262, USA*

Ethlene preferentially attacks the oxygen closest to the titanium in HOO–Ti(OSiH$_3$)$_3$(MeOH) and HOO–TiL$_3$ (MeOH) cluster models of the active Ti-site in TS1 due to a substantially reduced electrostatic repulsion.

Despite the advances and commercialization of TS-1 for alkene epoxidation with H_2O_2, the controlling mechanism has yet to be established. Clerici *et al.*,[1,2] and others[3,4] have speculated that the active intermediate in the epoxidation mechanism involves a five-membered ring structure similar to that shown (**I**). The solvent, here, is thought to act as a co-catalyst and stabilize the Ti–OOH intermediate. An alternative speculation is that the solvent helps solubilize the organic intermediate and the R–OH group depicted in **I** is a silanol group which could also stabilize the intermediate. The question then is which oxygen is attacked by the approaching alkene. While some have speculated that it is the oxygen O(2) in the terminal hydroxy group,[4,5] there is no experimental evidence to verify this.

Herein we use first-principle density-functional quantum chemical calculations to prove the nature of the active titanium site, examine the plausibility of the ROH stabilized reaction intermediate, and establish which of the oxygen atoms is preferentially attacked. While we specifically report on methanol as the ROH moiety in structure **I**, we find similar results for silanol.

Nonlocal density-functional theory (DFT) calculations† were used to compute the electronic and geometric structures, as well as the corresponding energies of various titanium silicate clusters chosen as models of the active Ti-binding sites. All calculations were performed using the VWN[7] exchange-correlation potential for the local spin density. Nonlocal gradient corrections for exchange (Becke[8]) and correlation (Perdew[9]) were computed internal to each SCF cycle. Rigorous geometry optimizations and second-derivative force constant calculations were performed to validate all minimum energy structures.

Various Ti(OSiH$_3$)$_x$ and TiL$_x$ clusters, where x varies from 3 to 6 and L is the specific ligand, were used to model adsorption sites in the zeolite framework. Hydrogen atoms were used to cap off all silicon atoms. The Ti–(OSiH$_3$)$_x$ cluster was used to determine adsorbate binding energies and reaction barriers, where x refers to varying number of siloxane groups. The TiL$_x$ structures were used to establish how changes in electronic substituents affect the charge at the Ti centre and adsorbate reactivity.

DFT-optimized tetrahedral, square-pyramidal, and octahedral structures consistent with known titanium silicates, bulk TiO$_2$ and SiO$_2$ were optimized. The results given in Table 1 are in excellent agreement with known experimental bond lengths established by EXAFS.[10–13] IR shifts for these structures are also in very good agreement with tabulated experimental spectra. The results clearly indicate bands at both 960 and 1000 cm^{-1} which correspond to SiO–H and Ti–O–Si asymmetric stretch modes, respectively. The experimental band at 960 cm^{-1}, which is a signature of the active titanium in different TS materials,[14] is still subject to considerable debate as to whether it is attributed to SiO$^-$ or Ti–O–Si (asymmetric) stretching modes. While the computed SiO–H band at 960 cm^{-1} matches the experimental value very well, the 40 cm^{-1} difference between the SiO–H and Ti–O–Si modes is within the 5% accuracy for DFT IR assignments and thus precludes a definitive answer. Both modes may, in fact, be present.

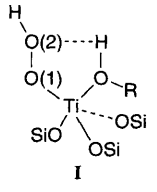

I

We have examined a set of plausible pathways for the epoxidation of the model alkene, ethene, by hydrogen peroxide in methanol over TS-1. The cycle contains four essential steps: the absorption of peroxide and methanol, the formation of the reactive hydroperoxy intermediate, the Ti-assisted epoxidation reaction, and the final desorption of products. We report on each of these steps in considerable detail in a forthcoming communication. The adsorption of peroxide and methanol act to initiate the cycle. Regardless of which of these occurs first, they both eventually lead to the reactive intermediate **I**. The peroxide is dissociated to form HOO–Ti–(OSiH$_3$)$_3$ and a neighbouring silanol (SiOH) fragment; methanol then adsorbs at the Ti-centre. The optimized HOO–Ti–(OSiH$_3$)$_3$–MeOH structure is shown in Fig. 1(*a*). The Ti–OOH bond is 1.45 Å, while the Ti bond to the oxygen of the methanol is, as expected, much longer (2.17 Å) and weaker. Hydrogen bonding between hydrogen on the methanol and the terminal OH group of the bound hydroperoxide enhances the stability of the intermediate as well as the transition state required to form the epoxide.

Ethene epoxidation was examined by bringing the ethene toward each of the two oxygens and rigorously optimizing the resulting geometries. Different approach paths for ethene attack at each oxygen centre were examined to verify whether bonding was possible.

The ethene interaction with the terminal OH oxygen, O(2), was found to be repulsive regardless of the direction of attack. Geometry optimization led to a positioning of the ethene moiety significantly removed (>3.5 Å) from the O(2) site as shown in Fig. 1(*b*). Ethene attack at the oxygen bound to the titanium

Table 1 Comparison of DFT-structure optimized and experimental titanium–oxygen bond lengths for titanium silicates in different coordination environments

Structure	DFT	Expt.	Ref.
Tetrahedral Ti(OSi)$_4$	1.81	1.80	10, 11
Trigonal-bipyramidal Ti(OSi)$_5$	1.84	—	
Square-pyramidal	1.68 Ti=O	1.65	
Ti=O(OSi)$_4$	1.96 av. Ti=O	1.96	12
Octahedral Ti(OSi)$_6$	1.96	1.95–2.00	10, 11
Tetrahedral SiO$_4$	1.65	1.615	13

O(1), on the other hand, was attractive and occurred through a back-side attack of ethene on the central oxygen O(1) of the –OOH group. The results indicate that as ethene approaches: (*i*) two C–O bonds are formed at the O(1) centre, (*ii*) the O–OH bond of the hydroperoxide group elongates, (*iii*) the terminal OH fragment from the hydroperoxide is stabilized by forming a bond with the OH hydrogen on methanol, and (*iv*) the O–H bond of silanol is subsequently weakened. The DFT-optimized reaction products are the epoxide, water and the tetrahedral $Ti(OSi)_3$–OMe moiety as depicted in Fig. 1(*c*). The epoxide remains attached to the Ti centre through a weak van der Waals interactions (23 kJ mol^{-1}) as evident from the long Ti–O bond length of 2.45 Å. The Ti-bound methoxy group is bound quite strongly and the DFT-computed Ti–O bond (1.84 Å) agrees quite well with the experimental Ti–O values (1.81–1.83 Å) for different titanium alkoxide species.[15] Water, on the other hand, is very weakly coordinated to the methoxy intermediate *via* a single hydrogen bond. The overall epoxidation reaction step is highly exothermic and computed to be −220 kJ mol^{-1}.

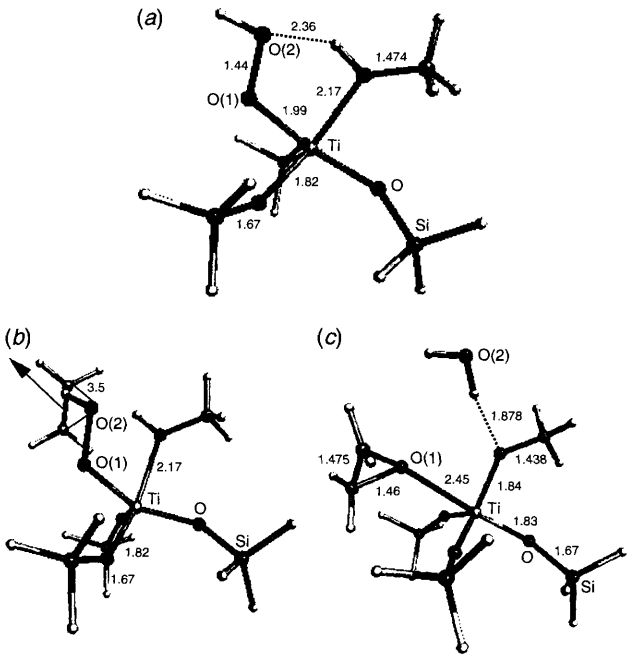

Fig. 1 DFT optimized structures for: (*a*) the proposed five-membered ring intermediate in titanium silicalite catalysed epoxidation in the presence of methanol [$Ti(OSiH_3)_3$–OMe–OOH], the result of ethene attack at (*b*) O(2) and (*c*) O(1) positions respectively. There is a repulsive interaction for attack at O(1) (*b*). Attack at O(2) results in the formation of the epoxide and water (*c*).

Table 2 Ligand effects on the epoxidation of ethene over TiL_3–OOH–MeOH. Comparison of DFT-computed Ti–epoxide bond lengths and Mulliken charges on the titanium and oxygen atoms for L = $–OSiH_3$, –F and –H

	Substituent		
Property	$OSi(H)_3$	F	H
Titanium charge	+1.31	+1.25	+0.23
Substituent charge	−0.65 (O)	−0.38 (F)	+0.03 (H)
O(epoxide) charge	−0.25	−0.32	−0.34
Ti–O (epoxide) bond length (Å)	2.5	2.25	2.15

The resulting electrostatic charge distribution helps to rationalize why O(1) is preferentially attacked. Both carbons on the incoming ethene fragment have a negative charge of −0.37 e. While both oxygens of the peroxide are negative, the charge on O(1) (−0.37) is much less negative than that on O(2) (−0.45). Repulsive forces are therefore significantly lower and much more easily overcome by attractive orbital overlap. Taking this a step further, we examined how changes in the substituents at the metal centre *i.e.* the $–(OSiH_3)_3$, could be manipulated to change the charge on O(1), and thus change product epoxide-binding and the rate of epoxide formation. The results are summarized in Table 2. The electron-withdrawing ability of the three Ti-ligand substituents rank in the following order: H < F < $OSiH_3$. The positive charge on the metal increases with increasing electron-withdrawing ability of the substituent. Subsequently the charge on the neighbouring O(1) atom becomes less negative. This reduces the repulsive interactions with ethene and thereby increases its ability to form the epoxide. In addition, the epoxide is more weakly bound. This is demonstrated by the increase in the Ti–epoxide product bond length with an increase in the substituent's electron-withdrawing potential.

In conclusion, calculations predict both the structure and relative bands in the IR spectra for titanium silicate structures to within very good agreement of experiment. The calculations indicate that oxygen closest to the titanium centre is the active site for alkene attack. The result is the direct formation of water, the regeneration of the tetrahedral Ti centre, and a weakly bound epoxide product. Substituent effects suggest that the reaction becomes more exothermic and releases the epoxide upon increasing the electron-withdrawing nature of the substituent.

We thank Dr Sourav Sengupta, Dr George W. Coulston, and Dr David A. Dixon from DuPont and Professor Robert J. Davis from the University of Virginia for their helpful discussions. M. N. thanks DuPont for their support and use of computational facilities.

References

1 G. Bellussi, A. Carati, M. G. Clerici, G. Maddinelli and R. Millini, *J. Catal.*, 1992, **133**, 220.
2 M. G. Clerici and P. Ingallina, *J. Catal.*, 1993, **140**, 71.
3 C. B. Khouw, C. B. Dartt, J. A. Labinger and M. E. Davis, *J. Catal.*, 1994, 149, **195**.
4 R. A. van Santen, *Theoretical Heterogeneous Catalysis*, World Scientific, Singapore, 1991.
5 M. G. Clerici and P. Ingallina, *J. Catal.*, 1993, **140**, 71.
6 J. Andzelm and E. Wimmer, *J. Chem. Phys.*, 1992, **96**, 1280.
7 S. H. Vosko, L. Wilk and M. Nusai, *Can J. Phys.*, 1980, **58**, 1200.
8 A. Becke, *J. Phys. Chem.*, 1988, **88**, 2547.
9 J. P. Perdew, *Phys. Rev. B.*, 1986, **33**, 8822.
10 Z. Liu and R. J. Davis, *J. Phys. Chem.*, 1994, **98**, 1253.
11 R. J. Davis, Z. Liu, J. E. Tabora and W. S. Wieland, *Catal.Lett.*, 1995, **34**, 101.
12 C. A. Yarker, P. A. V. Johnson, A. C. Wright, J. Wong, R. B. Greegor, F. W. Lytle and R. N. Sinclair, *J. Non-Cryst. Solids*, 1986, **79**, 117.
13 C. W. Earley, *Inorg. Chem.*, 1992, **31**, 1250.
14 G. Deo, A. M. Turek, I. Wachs, D. R. C. Huybrechts and P. A. Jacobs, *Zeolites*, 1993, **13**, 365.
15 F. Babonnea, S. Doeuff, A. Leaustic, C. Sanchez, C. Cartier and M. Verdaguer, *Inorg. Chem.*, 1988, **27**, 3166.

Received, 3rd January 1996; Com. 6/00053C